Electronic Supplementary Material (ESI) for Physical Chemistry Chemical Physics.

Supplementary Information

Effect of Annealing Temperature and Capping Ligands on the Electron Mobility and Electronic Structure of Indium Oxide Nanocrystals Thin Films: A Comparative Study with Oleic Acid, Benzoic Acid, and 4-Aminobenzoic Acid

Quang Trung Le, Hyeok Yun, Hyeonbeom Park and Hyun-Dam Jeong*

Department of Chemistry, Chonnam National University, Gwangju, 500-757, Republic of Korea

Result and discussion

- **Electron mobility**. As the thickness of the film increases, the electron mobility also improves. This phenomenon was studied in Ref.S1. According to their findings, it's primarily due to the reduction in the interface trap free energy of the film. In our experiments, we observed that as the annealing temperature of the thin film increased, the bonding between nanocrystals intensified, leading to a reduction in film thickness. This phenomenon is believed to be predominantly due to cross-linking among ligands or the connection between nanocrystal cores as a result of ligand decomposition at higher temperatures. Interestingly, even with these changes, there was a trend of increasing mobility. We attribute this to the enhanced connections between crystals, which likely increase the electronic coupling encountered by carriers during their movement. Additionally, it's worth noting that even if the thickness of the film decreases due to high-temperature annealing, the quantity of nanocrystals within the film is expected to remain consistent. Consequently, we did not factor in changes in film thickness in our calculations, as we deemed it appropriate to maintain consistency.
- **TEM**. Figure S1a shows the transmission scanning electron microscopy (TEM) image. The TEM image indicates highly spherical In_2O_3 nanocrystals (NCs) in samples. The size of the NCs was reduced due to surface etching (from 5.5±0.6 nm for OA-capped In_2O_3 NCs to 5.4±0.6 nm for BA-capped In_2O_3 NCs and 5.3±0.6 nm for 4ABA- capped In_2O_3 NCs) during the ligand-exchange process in the presence of nitric acid (HNO_3).
- **^{1}H NMR of indium oxide capped with oleic acid and ligand exchange (benzoic acid and 4-amino benzoic acid).** The chemical structure of surface capping groups of indium oxide NCs was characterized by ^{1}H NMR spectroscopy, compared with oleic acid, benzoic

acid, and 4-aminobenzoic acid-free molecules in Figure S1b. For OA-capped In_2O_3 NCs, chemical shift and assignments were as follows: 2.28-2.1 ppm (proton of H17), 1.56-1.49 ppm (proton of H16), and 5.28 ppm (-HC=CH-), 1.95 ppm (protons of H8 and H11), 1.20-1.22 ppm (protons of H3-7 and H12-15), 0.81 ppm (proton of H1) from oleate carboxylic groups. For BA-capped In_2O_3 NCs, chemical shift and assignments were as follows: 7.79 ppm (proton of H3) and 7.69 ppm (proton of H2). In the case of 4ABA-capped In_2O_3 NCs, chemical shift and assignments were as follows: 7.78 ppm ((proton of H2), 6.70 ppm ((proton of H1), and 6.05 ppm ((proton of H3). The chemical shift at 13.49 ppm (OH) for benzoic acid and at 12.41 ppm (-OH) for 4-aminobenzoic acid (DMF-D_4 as the solvent) disappeared on BA-capped In_2O_3 and 4ABA-capped In_2O_3 NCs, respectively. Thus, from the results of ^1H NMR spectroscopy, we determined that a complete ligand exchange reaction occurred.

Figure S1. a) The TEM image and size histogram illustrating the narrow size distribution of OA-capped In_2O_3, BA-capped In_2O_3, and 4ABA-capped In_2O_3 NCs. b) ^{1}H-NMR of In_2O_3 NCs and capping ligands.

Figure S2. Resonance contributors for 4-aminobenzoic acid protonated at (a) the carboxylic acid or (b) the amine. Reprinted with permission from ref. 1. Copyright 2012 American Chemical Society.

Figure S3. Raman spectrum of 4ABA-capped In_2O_3 NCs thin film was cured at 150, 200, and 250 ℃ in a vacuum.

Figure S4. Simple illustration of converting the CV graph to the DOS graph

Figure S5. Simple illustration of converting the ER-EIS graph to the DOS graph

Table S1. The molar ratios of substances used in manufacturing In_2O_3 NCs

Figure S1.

a)

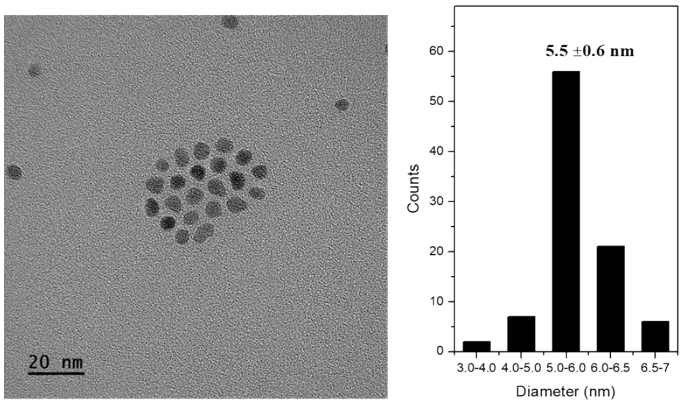

OA-capped In_2O_3 NCs

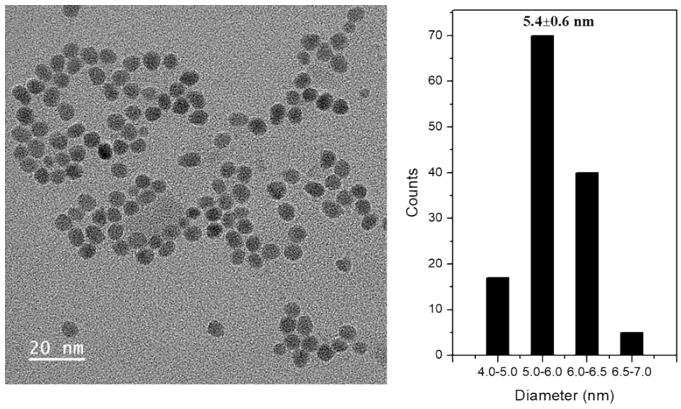

BA-capped In_2O_3 NCs

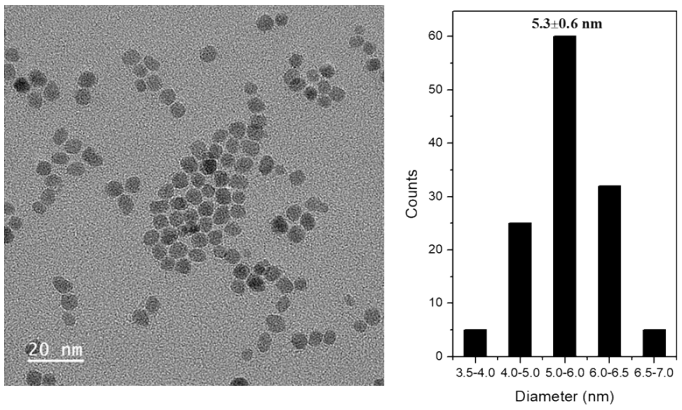

4ABA-capped In_2O_3 NCs

Figure S1.

b)

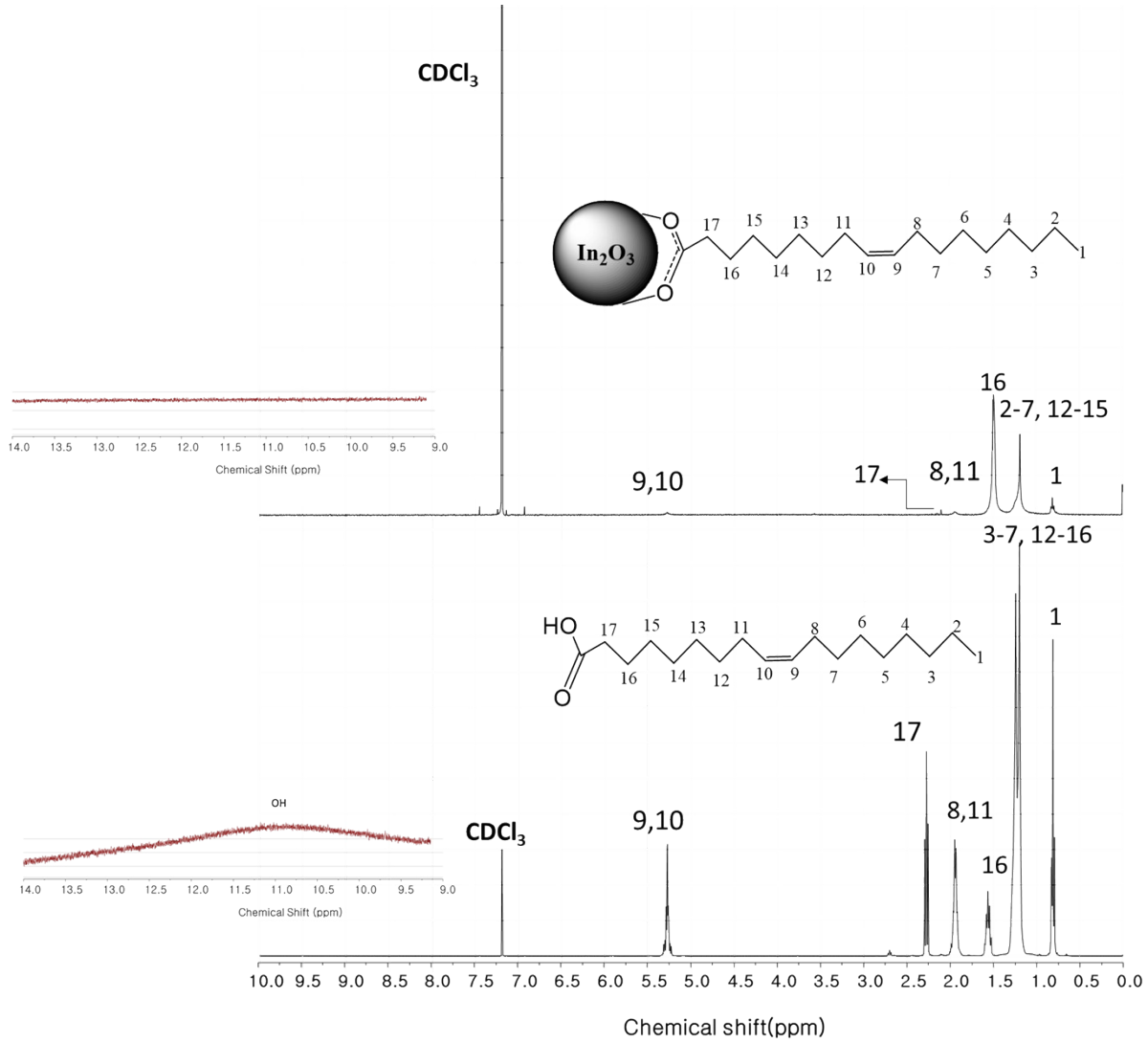

OA-capped In_2O_3 NCs and Olecic acid

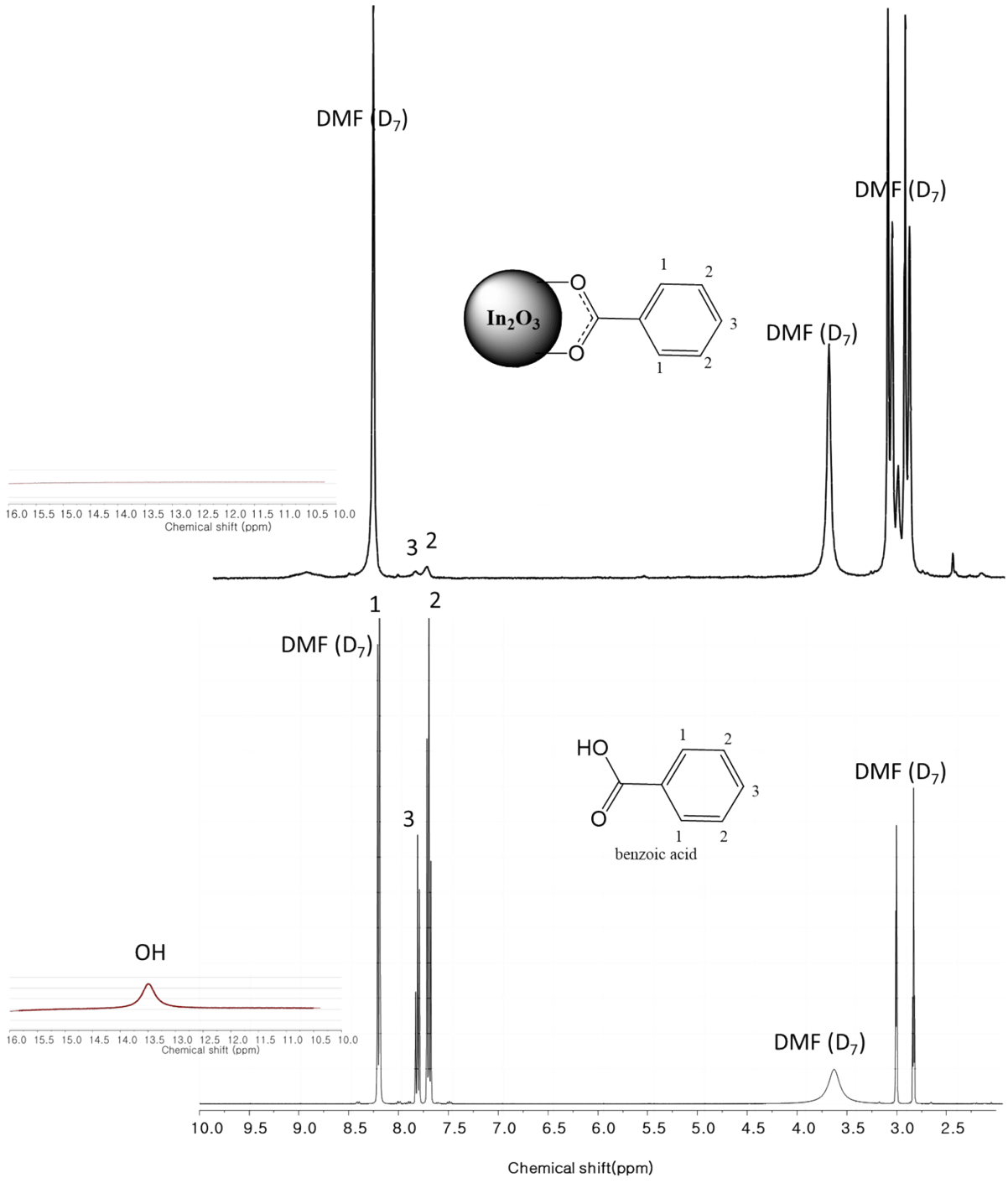

BA-capped In_2O_3 NCs and Benzoic acid

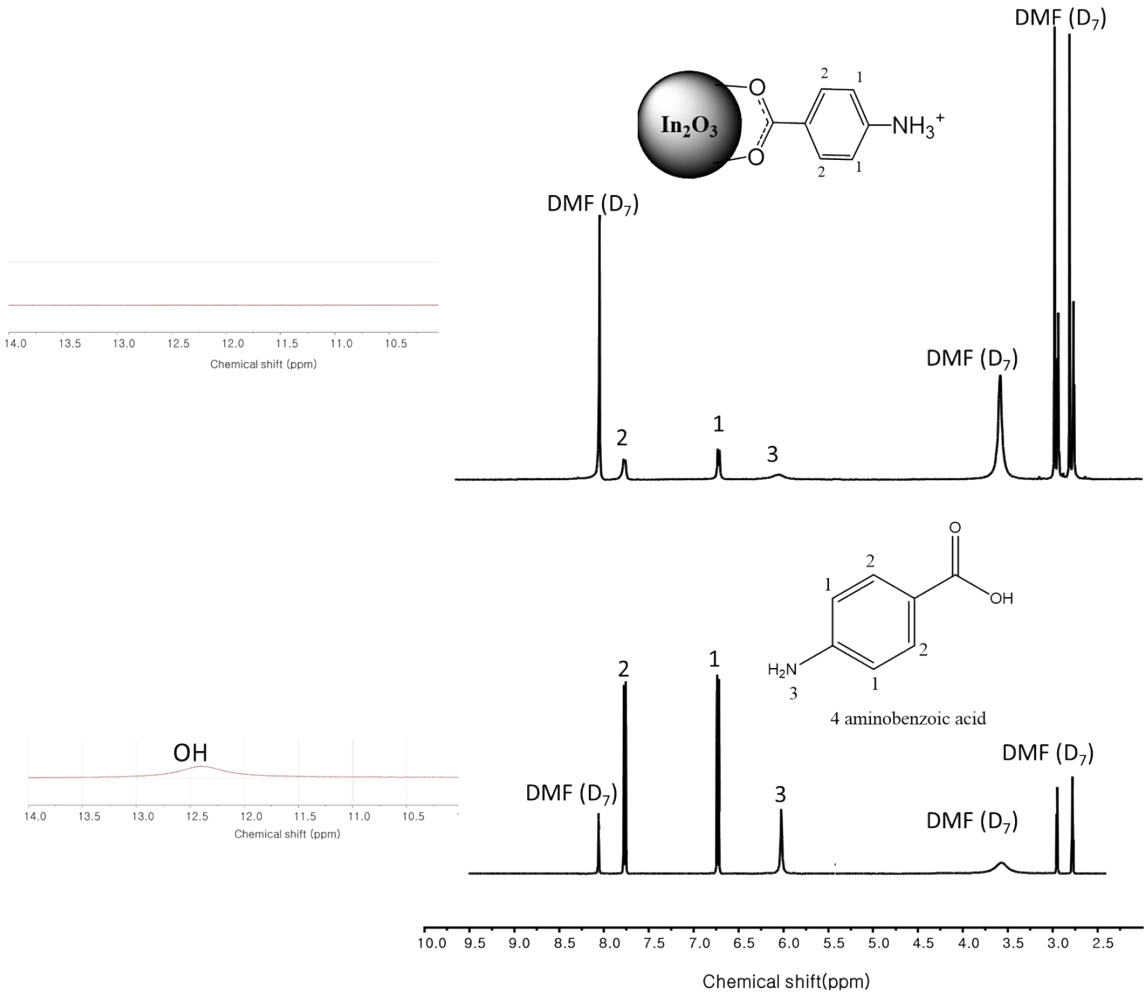

4ABA-capped In_2O_3 NCs and 4-aminobenzoic acid

Figure S2.

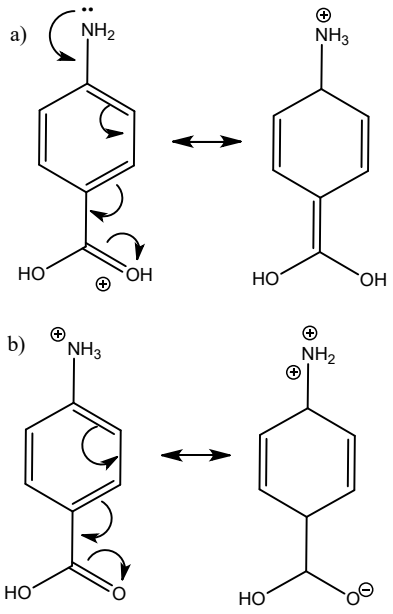

A neutral amine can donate electron density into the conjugated π system to better stabilize the positive charge associated with the protonated carboxylic acid (Figure S4a). If the amine is protonated, the carboxylic acid withdraws electron density due to the electronegativity of the oxygen atom, which destabilizes the positive charge at the protonated amine group (Figure S4b).[S2] In the case of 4ABA-capped In_2O_3 NCs thin films, the amine is protonated by nitric acid; thus, the stabilization of the protonated amine group is decreased. Therefore, we speculated that 4ABA-capped In_2O_3 NCs might reduce the system's energy by clustering together, diminishing the bandgap energy. This leads to a difference in bandgap between BA-capped In_2O_3 NCs and 4ABA-capped In_2O_3 NCs thin films.

Figure S3.

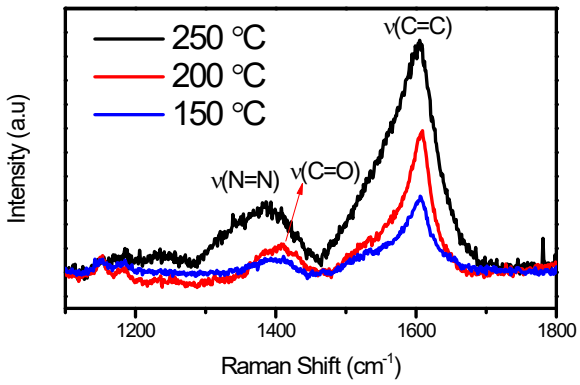

Raman spectrum (Figure S5) of 4ABA-capped In_2O_3 NCs thin film was cured at 150, 200, and 250 °C in a vacuum showing a band at 1604 cm^{-1}, attributed to the axial deformation C=C groups in an aromatic ring.[S3] Even when the annealing temperature is controlled to 250 °C, the C=C group does not disappear. Significantly, the stretching vibration of (ν(N=N)) at 1390 cm^{-1} is observed when the curing temperature is 250 °C,[S4] implying the amine groups in 4-aminobenzoic acid In_2O_3-$COOC_6H_5NH_2$ is oxidized to In_2O_3-$COOC_6H_5N{=}NC_6H_5COOIn_2O_3$. Based on the appearance of the N=N bonds, the electronic coupling of 4ABA-capped In_2O_3 NCs thin film to more convenient and faster than BA-capped In_2O_3 NCs.

Figure S4.

1) Conduct CV measurement.

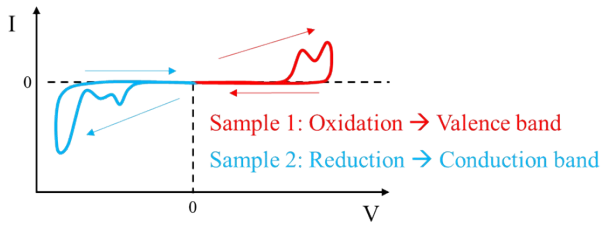

2) Extract half of the CV cycle.

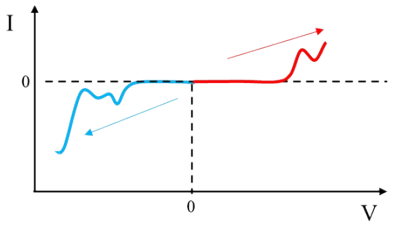

3) Vertically flip the reduction portion.

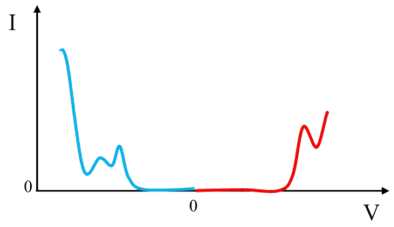

4) Horizontally flip the graph.

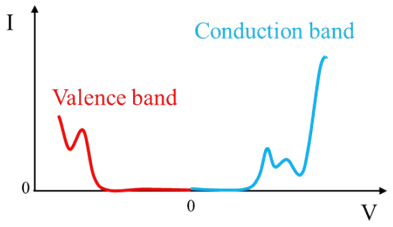

5) Adjust the potential
(according to the reference electrode.)

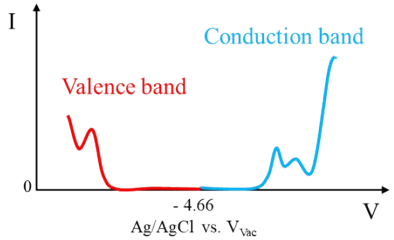

6) Convert the notation from I to DOS and from V to eV

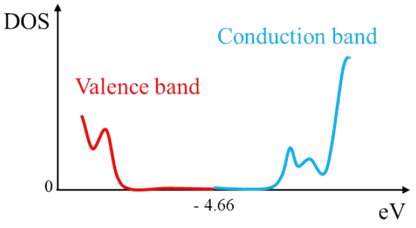

Figure S5.

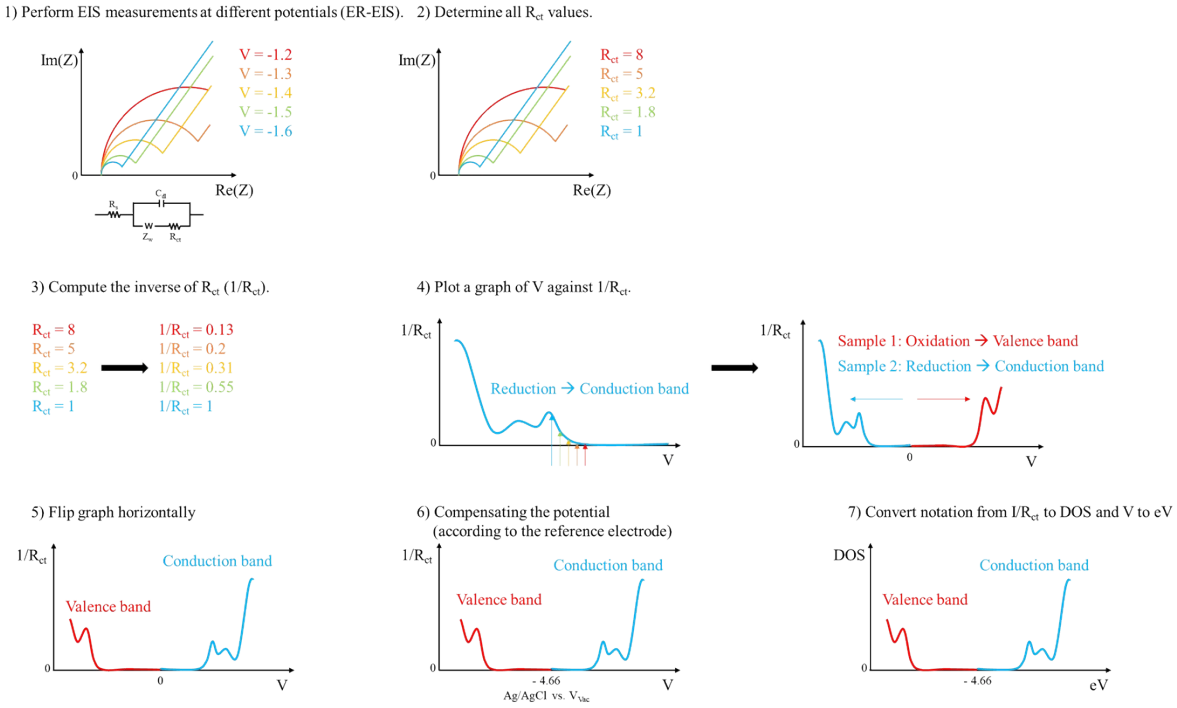
1) Perform EIS measurements at different potentials (ER-EIS).
2) Determine all R_{ct} values.
Im(Z)
Re(Z)
0
V = -1.2
V = -1.3
V = -1.4
V = -1.5
V = -1.6
C_{dl}
R_s
W
Z_w
R_{ct}
R_{ct} = 8
R_{ct} = 5
R_{ct} = 3.2
R_{ct} = 1.8
R_{ct} = 1
3) Compute the inverse of R_{ct} ($1/R_{ct}$).
$1/R_{ct}$ = 0.13
$1/R_{ct}$ = 0.2
$1/R_{ct}$ = 0.31
$1/R_{ct}$ = 0.55
$1/R_{ct}$ = 1
4) Plot a graph of V against $1/R_{ct}$.
$1/R_{ct}$
Reduction → Conduction band
V
Sample 1: Oxidation → Valence band
Sample 2: Reduction → Conduction band
5) Flip graph horizontally
Conduction band
Valence band
6) Compensating the potential
(according to the reference electrode)
- 4.66
Ag/AgCl vs. V_{vac}
7) Convert notation from I/R_{ct} to DOS and V to eV
DOS
eV

Table S1.

Material	ODA	ODE	ODE	$In(Ac)_3$	OA
Mass or volume	25.45 g	150 mL	12.5 mL	0.86 g	2.7 g
Amount of substance	94.1 mmol	469 mmol	39.1 mmol	2.95 mmol	9.56 mmol
ratio	1 : 5		40 : 3 : 10		

References

(S1) H. Xu, W. J. Zhai, C. Tang, S. Y. Qiu, R. L. Liu, Z. Rong, Z. Q. Pang, B. Jiang, J. Xiao, C. Zhong, B. X. Mi, Q. L. Fan and W. Hwang, Thickness Dependence of Carrier Mobility and the Interface Trap Free Energy Investigated by Impedance Spectroscopy in Organic Semiconductors, *J. Phys. Chem. C*, 2016, **120**, 17184-17189.

(S2) T. M. Chang, J. S. Prell, E. R. Warrick and E. R. Williams, Where's the Charge? Protonation Sites in Gaseous Ions Change with Hydration. *J. Am. Chem. Soc.* 2012, **134**, 15805-15813.

(S3) N. A. G. Gomez, S. A. Maruyama, A. Leuteritz and F. Wypych, Composites of polyethylene and layered cobalt hydroxide salts as potential ultraviolet radiation absorbers. *Polym. Bull.* 2020, **77**, 255-273.

(S4) X. Yan, L. Wang, X. Tan, B. Tian and J. Zhang, Surface-enhanced raman spectroscopy assisted by radical capturer for tracking of plasmon-driven redox reaction. *Sci. Rep*., 2016, **6**, 30193.